

Perylene Salts with Tetrahalogenoferrate(III) Anions. Synthesis, Crystal Structure of $[(C_{20}H_{12})_3][FeCl_4]$ and Characterisation†

José A. Ayllón,^a Isabel C. Santos,^a Rui T. Henriques,^a Manuel Almeida,^{*a} Elsa B. Lopes,^a Jorge Morgado,^b Luís Alcácer,^b Luís F. Veiros^b and M. Teresa Duarte^b

^a Departamento de Química, Instituto Tecnológico e Nuclear, P-2686 Sacavém Codex, Portugal

^b Instituto Superior Técnico, P-1096 Lisboa Codex, Portugal

Two new perylene ($C_{20}H_{12}$) salts $[(C_{20}H_{12})_3][FeCl_4]$ **1** and $[(C_{20}H_{12})_3][FeBr_4]$ **2** have been synthesised and characterised. Compound **1** crystallises in the triclinic system, space group $P\bar{1}$, with $a = 12.8393(11)$, $b = 14.1333(11)$, $c = 14.8391(14)$ Å, $\alpha = 91.680(7)$, $\beta = 113.114(7)$, $\gamma = 115.119(7)$ and $Z = 2$, and its structure consists of tetramerised stacks of perylenes flanked by additional pseudo-orthogonal perylene molecules and tetrachloroferrate(III) anions. Resistivity and thermopower measurements characterise $[(C_{20}H_{12})_3][FeCl_4]$ **1** as a semiconductor with a room-temperature conductivity $\sigma \approx 0.17$ S cm^{-1} with an activation energy of 0.12 eV. The magnetic behaviour of both compounds is dominated by the contribution of the paramagnetic iron(III) centres. Magnetic susceptibility data in the temperature range 3–300 K were fitted to the equation for a binuclear $S = S' = \frac{5}{2}$ interaction, with $J/k = -1.26(1)$ K and $g = 2.022(4)$ for **1** and $J/k = -3.72(4)$ K and $g = 2.03(2)$ for **2**.

During the last two decades molecular conductors have been the subject of intensive studies and many conducting and even superconducting systems have been extensively characterised, establishing the basic rules for electronic transport in molecular solids. However, despite this extensive research, the properties derived from the coexistence of conduction electrons and paramagnetic centres in molecular solids have remained virtually unexplored. The challenge of the preparation of a molecular solid exhibiting both superconductivity and ferromagnetism only recently has been achieved for κ -[betff]₂[Cu{N(CN)₂}Cl]¹ [betff = bis(ethylenedithio)tetrathiafulvalene, tetrathiafulvalene = 2-(1',3'-dithiol-2'-ylidene)-1,3-dithiole] while the incorporation of a paramagnetic centre in a molecular conductor has been successfully studied in only a few cases.

Perylene ($C_{20}H_{12}$) is one of the earliest organic molecules known as able to provide conducting properties.² The $[(C_{20}H_{12})_3][M(mnt)_2]$ family of compounds (H_2mnt = maleo-nitriledithiol or *cis*-2,3-disulfanylbut-2-enedinitrile) has been intensively studied in our laboratory^{3–7} since the first report of compounds of this type with $M = Cu^{III}$, Ni^{III} or Pd^{III} .⁸ For $M = Ni^{III}$, Pd^{III} , Pt^{III} or Fe^{III} , the $M(mnt)_2$ units are paramagnetic and as a consequence these compounds present unique properties derived from the coexistence of conducting perylene and magnetic $M(mnt)_2$ chains in the same solid. Some of these properties resemble those of $Cu(pc)I$ (pc = phthalocyaninate), the interaction of conduction electrons and localised spins is also evident.^{9,10} More recently the properties of betff salts with different paramagnetic metal complexes has been also investigated.¹¹

As part of an effort to obtain new perylene based molecular conductors with paramagnetic counter ions we have recently synthesised new compounds containing tetrahalogenoferrate(III) $S = \frac{5}{2}$ anions. In this paper the preparation and characterisation of $[(C_{20}H_{12})_3][FeX_4]$ ($X = Cl$ or Br) are reported.

Experimental

Synthesis and Electrocrystallisation.—The starting reagents were carefully purified. Perylene (Sigma) was twice gradient sublimed [10^{-2} Torr (*ca.* 1.33 Pa), 110 °C] after recrystallisation from pentane and alumina-silica chromatography.¹² Tetraalkylammonium salts of the anions FeX_4^- (NEt_4^+ for $X = Cl$ and NBu_4^+ for $X = Br$) were prepared from ethanolic solutions of the corresponding metal and tetraalkylammonium halides. The resulting precipitates were recrystallised from hot ethanol.

$[(C_{20}H_{12})_3][FeCl_4]$ **1**. Single crystals were prepared by electrochemical oxidation of perylene in a 1,1,2-trichloroethane solution ($\approx 10^{-2}$ mol dm^{-3}) saturated with $NEt_4[FeCl_4]$. The electrocrystallisation was performed in a two-compartment cell on platinum electrodes through a galvanostatic technique,¹³ using current densities in the range 2–10 μA cm^{-2} . Elemental analyses were obtained using a Perkin-Elmer 240 elemental analyser at the analytical service of the Instituto Tecnológico e Nuclear (Found: C, 75.4; H, 3.7. $C_{60}H_{36}Cl_4Fe$ requires C, 75.5; H, 3.8%).

$[(C_{20}H_{12})_3][FeBr_4]$ **2** was obtained in a similar procedure starting from a dichloromethane solution of perylene ($\approx 10^{-2}$ mol dm^{-3}) saturated with $NBu_4[FeBr_4]$ (Found: C, 63.5; H, 3.1. $C_{60}H_{36}Br_4Fe$ requires C, 63.6; H, 3.2%).

X-Ray Crystallography.—The crystal was mounted in a glass capillary on a goniometer head. X-Ray data were collected at room-temperature on an Enraf-Nonius CAD-4 automatic diffractometer by using graphite-monochromated $Mo-K\alpha$ ($\lambda = 0.71069$ Å) radiation. Unit-cell dimensions and the crystal orientation matrix were obtained from least-squares refinement of the setting angles of 25 reflections in the range $10 < \theta < 17^\circ$. The unit cell was identified as triclinic, space group $P\bar{1}$. This choice was confirmed by the solution and the successful refinement of the structure. The data set was collected in the ω - 2θ scan mode [$\Delta\omega = (0.80 + 0.35 \tan \theta)^\circ$]. The intensities were corrected for Lorentz, polarisation and absorption effects by empirical corrections based on ψ -scans (maximum and minimum transmission factors were 0.998 and 0.974), using the Enraf-Nonius program. The structure was solved by direct

† Supplementary data available: see Instructions for Authors, *J. Chem. Soc., Dalton Trans.*, 1995, Issue 1, pp. xxv–xxx.

Non-SI units employed: emu = SI $\times 10^6/4\pi$; eV $\approx 1.6021 \times 10^{-19}$ J, $\mu_B \approx 9.274 \times 10^{-24}$ J T^{-1} ; G = 10^{-4} T.

methods using SHELX 86,^{14a} and subsequently completed by Fourier recycling, using SHELXL 93.^{14b} All non-hydrogen atoms were refined anisotropically. The hydrogen atoms were

Table 1 Complete crystallographic data for [(C₂₀H₁₂)₃][FeCl₄]

| | |
|---|--|
| Formula | C ₆₀ H ₃₆ Cl ₄ Fe |
| M _w | 954.54 |
| Crystal system | Triclinic |
| Space group | P $\bar{1}$ |
| a/Å | 12.8393(11) |
| b/Å | 14.1333(11) |
| c/Å | 14.8391(14) |
| α/° | 91.680(7) |
| β/° | 113.114(7) |
| γ/° | 115.119(7) |
| U/Å ³ | 2179.4(3) |
| Z | 2 |
| D _c /Mg m ⁻³ | 1.455 |
| F(000) | 980 |
| T/K | 293(2) |
| λ/Å | 0.710 69 |
| μ(Mo-Kα)/mm ⁻¹ | 6.35 |
| 2θ/° | 3.08–55.92 |
| Index ranges | –16 < h < 15, –18 < k < 18, 0 < l < 19 |
| Reflections collected | 10 885 |
| Independent reflections (R _{int} = 0.0356) | 10 484 |
| Data/restraints/parameters | 10 484/0/587 |
| R ^a | [F _o > 4σ(F _o)] 0.0649 |
| R ^b | 0.1040 |
| Goodness-of-fit, S ^c | 0.795 |
| Largest difference peak and hole/e Å ⁻³ | 0.270, –0.270 |

^a $R = \sum |F_o| - |F_c| / \sum |F_o|$. ^b $R' = \{ \sum [w(F_o - F_c)^2] / \sum [w(F_c)^2] \}^{1/2}$. ^c $S = \{ \sum [w(F_o - F_c)^2] / (n - p) \}^{1/2}$, $w = 1 / [\sigma^2(F_o) + (0.0442P)^2]$, $P = [\text{Max.}(F_o + 2F_c)]/3$, n = number of observations, p = number of parameters.

set in calculated positions. Final refinement on F_o by full-matrix least-squares techniques with anisotropic thermal displacement parameters for the non-hydrogen atoms converged at R = 0.0649 and R' = 0.1040 and S = 0.795. A difference Fourier synthesis revealed residual densities between –0.270 and 0.270 e Å⁻³. Crystallographic data and details of the structure refinement are reported in Table 1, final fractional atomic coordinates for non-hydrogen atoms are given in Table 2, and bond distances and bond angles for the FeCl₄⁻ anion are collected in Table 3. Scattering factors and anomalous dispersion factors used were those supplied in SHELX 93. All calculations were carried out on a μVAX3400 computer at the Instituto Superior Técnico, using SHELX,¹⁴ PARST¹⁵ (calculation of geometric data) and ORTEP II.¹⁶

Additional material available from the Cambridge Crystallographic Data Centre comprises H-atom coordinates, thermal parameters and remaining bond lengths and angles.

Electrical Transport Measurements.—Electrical conductivity measurements, along the needle axis *b* of (C₂₀H₁₂)₃FeCl₄ single crystals, were made in the temperature range 170–300 K using an in-line four-probe configuration and a low-frequency (77 Hz) current of 1 μA, the voltage being measured by a lock-in amplifier (EG&G PAR model 5301). Gold evaporated contacts on the sample were glued to 25 μm o.d. gold wires with platinum paint (Demetron 308A). This study was hampered with difficulties associated with the poor quality of the contacts as a consequence of the reactivity of the samples toward the conducting paint and sample fragility. In order to minimise these problems, it was essential to use evaporated gold pads and avoid placing any conducting paint outside the gold pads. Special care was taken to select samples with a low (<=10%) un-nested/nested voltage ratio as defined by Schaffer *et al.*¹⁷ The measurements were done in a closed-cycle cryostat (ADP Cryogenics Inc, HC-2/DE 202), and the temperature was

Table 2 Fractional atomic coordinates (×10⁴) for [(C₂₀H₁₂)₃][FeCl₄]

| Atom | x | y | z | Atom | x | y | z |
|--------|-----------|-----------|----------|--------|-----------|-----------|----------|
| Fe | 2 620(1) | 3 843(1) | 1 222(1) | C(9B) | 2 368(4) | 10 184(3) | 5 893(3) |
| Cl(1) | 3 846(1) | 4 508(1) | 2 853(1) | C(10B) | 1 083(3) | 9 418(3) | 5 285(3) |
| Cl(2) | 1 612(1) | 2 085(1) | 887(1) | C(11B) | 543(3) | 9 170(3) | 4 183(3) |
| Cl(3) | 1 229(1) | 4 443(1) | 666(1) | C(12B) | 1 245(4) | 9 659(3) | 3 675(3) |
| Cl(4) | 3 845(1) | 4 338(1) | 458(1) | C(13B) | 700(5) | 9 414(4) | 2 625(3) |
| C(1A) | 364(4) | 6 410(3) | 5 880(3) | C(14B) | –564(5) | 8 660(4) | 2 074(3) |
| C(2A) | –954(4) | 5 605(3) | 5 305(3) | C(15B) | –1 322(4) | 8 145(3) | 2 553(3) |
| C(3A) | –1 652(4) | 5 088(3) | 5 824(3) | C(16B) | –2 632(5) | 7 372(4) | 1 982(3) |
| C(4A) | –1 106(4) | 5 343(3) | 6 866(3) | C(17B) | –3 354(4) | 6 861(4) | 2 447(4) |
| C(5A) | 133(4) | 6 108(3) | 7 420(3) | C(18B) | –2 835(4) | 7 089(3) | 3 482(4) |
| C(6A) | 891(4) | 6 645(3) | 6 946(3) | C(19B) | –1 561(3) | 7 851(3) | 4 093(3) |
| C(7A) | 2 183(4) | 7 439(3) | 7 513(3) | C(20B) | –780(4) | 8 390(3) | 3 617(3) |
| C(8A) | 2 919(4) | 7 956(3) | 7 050(3) | C(1C) | 4 969(3) | 999(3) | 4 957(3) |
| C(9A) | 2 422(4) | 7 721(3) | 6 010(3) | C(2C) | 4 535(3) | 268(3) | 4 044(3) |
| C(10A) | 1 137(3) | 6 949(3) | 5 400(3) | C(3C) | 4 091(4) | 566(4) | 3 151(3) |
| C(11A) | 584(4) | 6 692(3) | 4 305(3) | C(4C) | 4 067(4) | 1 543(5) | 3 119(4) |
| C(12A) | 1 279(4) | 7 196(3) | 3 781(3) | C(5C) | 4 471(5) | 2 235(4) | 3 966(5) |
| C(13A) | 741(5) | 6 939(4) | 2 744(4) | C(6C) | 4 954(4) | 2 009(3) | 4 908(4) |
| C(14A) | –511(5) | 6 180(4) | 2 187(3) | C(7C) | 5 393(4) | 2 705(4) | 5 803(5) |
| C(15A) | –1 276(4) | 5 660(3) | 2 666(3) | C(8C) | 5 845(5) | 2 492(4) | 6 707(4) |
| C(16A) | –2 581(5) | 4 886(4) | 2 101(3) | C(9C) | 5 878(4) | 1 512(4) | 6 771(3) |
| C(17A) | –3 297(4) | 4 379(4) | 2 578(4) | C(10C) | 5 461(3) | 762(3) | 5 916(3) |
| C(18A) | –2 787(4) | 4 599(3) | 3 607(3) | C(1D) | 3 967(4) | –788(4) | 160(3) |
| C(19A) | –1 496(3) | 5 367(3) | 4 219(3) | C(2D) | 4 868(5) | –1 051(4) | 60(3) |
| C(20A) | –726(4) | 5 910(3) | 3 738(3) | C(3D) | 4 717(5) | –2 078(4) | 143(3) |
| C(1B) | 311(4) | 8 874(3) | 5 763(3) | C(4D) | 3 704(6) | –2 826(4) | 311(4) |
| C(2B) | –997(4) | 8 093(3) | 5 191(3) | C(5D) | 2 841(6) | –2 555(5) | 382(4) |
| C(3B) | –1 700(4) | 7 594(3) | 5 710(4) | C(6D) | 2 917(5) | –1 555(4) | 312(3) |
| C(4B) | –1 175(5) | 7 833(4) | 6 751(4) | C(7D) | 2 021(5) | –1 290(5) | 383(3) |
| C(5B) | 73(5) | 8 577(4) | 7 301(3) | C(8D) | 2 164(6) | –275(6) | 343(4) |
| C(6B) | 854(4) | 9 120(3) | 6 836(3) | C(9D) | 3 188(5) | 482(5) | 221(3) |
| C(7B) | 2 148(4) | 9 903(3) | 7 397(3) | C(10D) | 4 084(4) | 270(4) | 117(3) |
| C(8B) | 2 883(4) | 10 421(3) | 6 934(3) | | | | |

monitored by an Au (0.07 atom % Fe)–Chromel thermocouple placed close to the sample. The poorer quality and smaller dimensions of $[(C_{20}H_{12})_3][FeBr_4]$ crystals prevented either X-ray structure determination or electrical transport measurements.

The thermopower was measured, along the needle axis b of $[(C_{20}H_{12})_3][FeCl_4]$ single crystals, relative to gold, in the range 120–300 K, by a slow AC technique (10^{-2} Hz) in an apparatus similar to that described by Chaikin and Kwak¹⁸ placed inside the same closed-cycle helium cryostat. The thermal gradients used were <1 K, and they were monitored by an Au (0.07 atom % Fe)–Chromel thermocouple. Absolute thermopower was obtained after correction for the small gold absolute thermopower using the data of Huebner.¹⁹

Magnetic Susceptibility.—Magnetic susceptibility measurements were performed in the range 3–300 K using a Faraday System (Oxford Instruments) with a 7 T superconducting magnet using polycrystalline samples (≈ 10 mg for each compound) placed in previously measured thin-walled Teflon buckets. The magnetic fields used were 2 and 0.5 T, and the resulting force was measured with a microbalance (Sartorius S3D-V) applying forward and reverse gradients of 5 T m^{-1} . Under these conditions, the magnetisation was found to be proportional to the applied magnetic field. Paramagnetic susceptibility was calculated from the raw susceptibility data correcting for diamagnetism, which was estimated from tabulated Pascal's constants as $-6.14 \times 10^{-4} \text{ emu mol}^{-1}$ for **1** and $-6.58 \times 10^{-4} \text{ emu mol}^{-1}$ for **2**.

EPR.—Electron paramagnetic resonance spectra were obtained at room temperature with a conventional X-band spectrometer (Bruker ESP 300E). Single crystals were fixed to a signal-free Teflon holder with a minimum amount of Apiezon grease, which was placed inside a quartz tube, which in turn was placed inside the cavity. The g factors were determined by simultaneously measuring the microwave frequency (Bruker ER/041/XK frequency counter) and the magnetic field (ER035M NMR gaussmeter, Bruker).

Results and Discussion

The crystal structure of $[(C_{20}H_{12})_3][FeCl_4]$ consists of tetramerised stacks of perylene units along the b axis flanked by $FeCl_4^-$ anions and additional perylene units (Fig. 1). The unit cell contains four independent perylene species and one independent $FeCl_4^-$ anion. Two full perylene species (residues A and B) are at a general position and belong to the stacks. Two other half perylene units (residues C and D) are at inversion centres at $(0.5, 0, 0.5)$ and $(0.5, 0, 0)$ respectively, and are almost perpendicular to the stacked ones. The $FeCl_4^-$ anion is also at a general position. The four perylene units are planar and present, within experimental uncertainty, the same bond distances and angles. The charge balance imposes a positive charge among the perylene units. As in many other charge-transfer complexes based on large aromatic hydrocarbons, no information about the charge distribution can be obtained from the bond distances and angles. However, as it will be discussed later, transport properties suggest the existence of the $(C_{20}H_{12})_2^+$ cation in the stacks. Consequently the perylene species at C and D would be neutral molecules.

Table 3 Bond distances (Å) and angles ($^\circ$) for the $FeCl_4^-$ anion in **1**

| | | | |
|----------------|------------|----------------|------------|
| Fe–Cl(1) | 2.1996(12) | Fe–Cl(3) | 2.1811(13) |
| Fe–Cl(2) | 2.1884(13) | Fe–Cl(4) | 2.1812(12) |
| Cl(3)–Fe–Cl(4) | 109.09(5) | Cl(3)–Fe–Cl(1) | 110.68(5) |
| Cl(3)–Fe–Cl(2) | 109.85(6) | Cl(4)–Fe–Cl(1) | 108.43(5) |
| Cl(4)–Fe–Cl(2) | 108.44(5) | Cl(2)–Fe–Cl(1) | 110.30(5) |

The perylene stacks, consisting in the repeat $B-A-A^1-B^1$ ($I-x, 1-y, 1-z$), are well separated both by the anions and the perylene molecules C and D (Fig. 2). The stacking and their packing is very similar to $[(C_{20}H_{12})_2]PF_6 \cdot \frac{1}{2} \text{thf}$ (thf = tetrahydrofuran) although quite different from the compound $[(C_{20}H_{12})_3]ClO_4$,²⁰ in spite of having the same stoichiometry and an anion with the same symmetry.

The perylene units A and B are parallel within experimental uncertainty (their normals make an angle of $\approx 0.5^\circ$) and are roughly perpendicular to the C and D molecules that flank the stack (angles A–C, 72.73° , A–D, 88.59°). The angle between perylene molecule C and perylene molecule D is 78.51° . The perylene species in the stacks have a normal at *ca.* 17° to the b axis (A, 17.58° , B, 17.05°). Within the stack the three crystallographically independent interplanar distances, A–B and A–A¹ 3.38, B–B¹¹ 3.37 Å ($II-x, 2-y, 1-z$), are almost identical but the perylene overlap modes are significantly different as shown in Fig. 3. The overlap mode A–B is characterised by a slip along the short molecular axis of the perylene molecule. The slip in the A–A¹ overlap has also a small component in the direction of the major axis. In the third overlap mode, B–B¹¹, the slip has similar components along the two axes. Therefore the perylene stacks are tetramerised, due to a transversal modulation of the chains, at variance with $[(C_{20}H_{12})_3]ClO_4$ which presents a tetramerisation due to a strong longitudinal modulation.

The $FeCl_4^-$ anion presents a geometry close to ideal tetrahedral, the Fe–Cl bond lengths ranging from 2.181(1) to 2.200(1) Å (average 2.188 Å), comparable to the reported Fe–Cl distances in other $FeCl_4^-$ containing structures.²¹ The Cl–Fe–Cl angles, ranging from $108.43(5)$ to $110.68(5)^\circ$, indicate a very slight distortion of the ideal tetrahedral geometry.

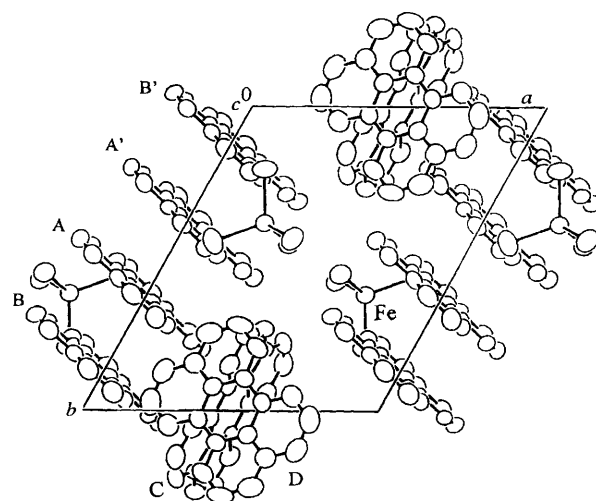


Fig. 1 ORTEP projection along the c axis of the $[(C_{20}H_{12})_3][FeCl_4]$ crystal structure. Hydrogen atoms are omitted for clarity

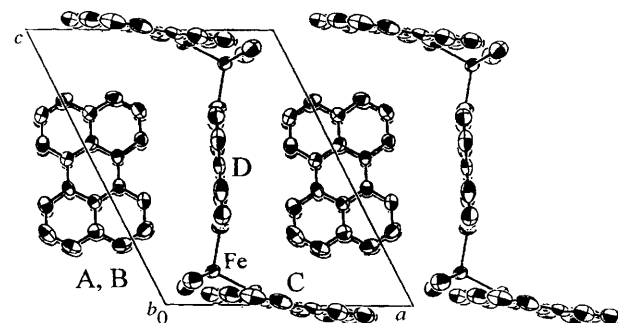


Fig. 2 ORTEP projection along the b axis of the $[(C_{20}H_{12})_3][FeCl_4]$ structure. Hydrogen atoms are omitted for clarity

The FeCl_4^- anion has interactions with neighbouring species, although the closest separation between two FeCl_4^- corresponds to an $\text{Fe} \cdots \text{Fe}^{\text{III}}$ separation of 7.89 Å (III 1 - x , 1 - y , - z). The Fe-Cl(4) bond is almost collinear with the $\text{Fe} \cdots \text{Fe}^{\text{III}}$ axis and the Cl(4) \cdots Cl(4^{III}) distance, 3.571 Å, is slightly less than the sum of the van der Waals radii (3.6 Å). This almost collinear geometry $\text{Fe}-\text{Cl}(4) \cdots \text{Cl}(4^{\text{III}})-\text{Fe}^{\text{III}}$ (Fig. 4) is not expected to be stable, unless if driven by other dominating interactions. This is indeed the case in this crystal structure where important interactions between the FeCl_4^- anions and the perylene molecules exist, as denoted by several $\text{Cl} \cdots \text{H}$ distances below or in the range of the sum of the van der Waals radii, as listed in Table 4.

The electrical conductivity of $[(\text{C}_{20}\text{H}_{12})_3]\text{FeCl}_4$, **1**, measured along the needle axis b is 0.17 S cm^{-1} at room temperature, and has a thermally activated behaviour typical of a semiconductor, with an activation energy of 0.12 eV at room temperature (Fig. 5). Below 255 K there is a decrease of the activation energy towards 0.08 eV.

The thermopower, S , of **1**, measured along the needle axis b , is positive in the whole temperature range covered, indicating a hole-dominated transport, with a room-temperature value of $S(300 \text{ K}) = 275 \mu\text{V K}^{-1}$. Its temperature dependence also indicates a semiconducting behaviour in agreement with conductivity data. As shown in Fig. 6, S plotted versus $1/T$ shows straight line behaviour typical of semiconductors, but with a change of slope at ca. 235 K, approximately the same temperature where a change in the activation energy of conduction was observed. The origin of the slope change around this temperature can be a gap variation induced by a possible structural change.

The thermopower for a semiconductor with a gap 2Δ is expected to obey equation (1)²² where b is the hole to electron

$$S = a + \left(\frac{b-1}{b+1} \right) (\Delta/kT) \quad (1)$$

mobility ratio: $b = \mu^+/\mu^-$. While for low temperatures the S vs. $1/T$ slope gives $[(b-1)/(b+1)] \Delta/k = 0.07 \text{ eV}$, a value that is smaller but close to the activation energy derived from conductivity, $\Delta = 0.08 \text{ eV}$, indicating a mobility ratio of $b \approx 15$, the high-temperature S vs. $1/T$ slope approaches 0.23 eV, a value larger than the one obtained from conductivity, indicating that the gap or the mobility ratio are not temperature independent in this temperature range.

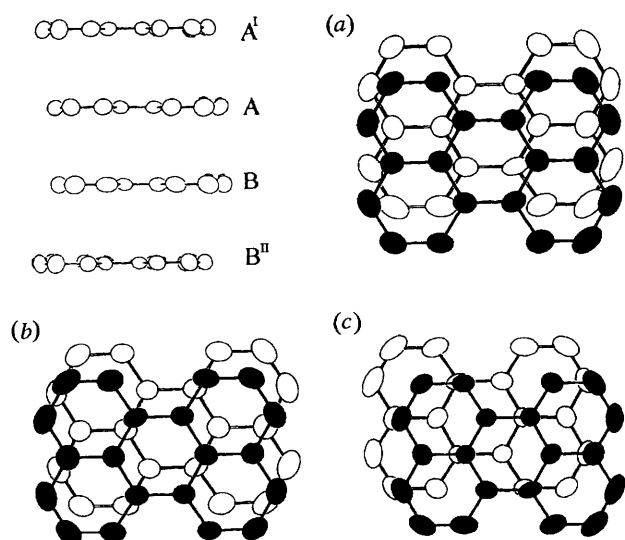


Fig. 3 Overlap modes within the perylene stacks: (a) A-B, (b) A-A', (c) B-B''

The magnetic susceptibilities of both compounds are relatively large [$\chi_p(300 \text{ K}) = 0.016 \text{ emu mol}^{-1}$ (in SI units: $2.01 \times 10^{-7} \text{ m}^3 \text{ mol}^{-1}$) for **1** and $0.015 \text{ emu mol}^{-1}$ (in SI units: $1.88 \times 10^{-7} \text{ m}^3 \text{ mol}^{-1}$) for **2**] indicating that they are dominated by the contribution of the $S = \frac{5}{2} \text{ Fe}^{\text{III}}$ centres. The paramagnetic susceptibility, χ_p , obtained for compounds **1** and **2** as a function of temperature is plotted in Fig. 7. In both compounds χ_p closely follows a Curie-Weiss law, $\chi_p = C/(T - \theta)$, above 25 K for **1** and 55 K for **2**, with negative Weiss constants, $\theta = -12.1(2) \text{ K}$ for **1** and $\theta = -39.9(6) \text{ K}$ for **2**. The Curie constants [$C = 4.81(1)$ for **1**, $5.14(1) \text{ emu K mol}^{-1}$ for **2**] correspond to an effective magnetic moment of $6.21 \mu_B$ and $6.4 \mu_B$, close to the spin-only value predicted for a high spin $3d^5 \text{ Fe}^{3+}$ with $S = \frac{5}{2}$ ($5.92 \mu_B$). The slightly higher effective magnetic moment could be due to some ferromagnetic trace impurities. The negative Weiss constants denote antiferromagnetic interaction between spins. These interactions are also denoted by maxima in the paramagnetic susceptibility, close to 7 and 21 K for **1** and **2** respectively.

Table 4 Hydrogen-chloride distances (Å) < 3.15 Å in **1**

| | | | |
|-----------------------------|-------|-----------------------------|-------|
| Cl(4)-H(16B ^{IV}) | 2.846 | Cl(3)-H(4A ^I) | 3.057 |
| Cl(4)-H(17B ^V) | 2.985 | Cl(2)-H(14B ^{IV}) | 3.098 |
| Cl(1)-H(5C) | 3.029 | Cl(4)-H(16A ^{IV}) | 3.115 |
| Cl(2)-H(4B ^I) | 3.035 | Cl(2)-H(8D) | 3.118 |
| Cl(3)-H(14A ^{IV}) | 3.045 | Cl(1)-H(7C ^{VI}) | 3.123 |
| Cl(1)-H(4B ^I) | 3.051 | Cl(2)-H(4C) | 3.123 |

Symmetry operations: I - x , 1 - y , 1 - z ; IV - x , 1 - y , - z ; V 1 + x , y , z ; VI 1 - x , 1 - y , 1 - z .

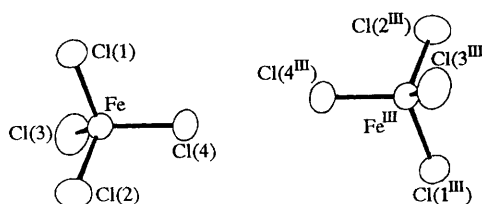


Fig. 4 Nearest FeCl_4 pair

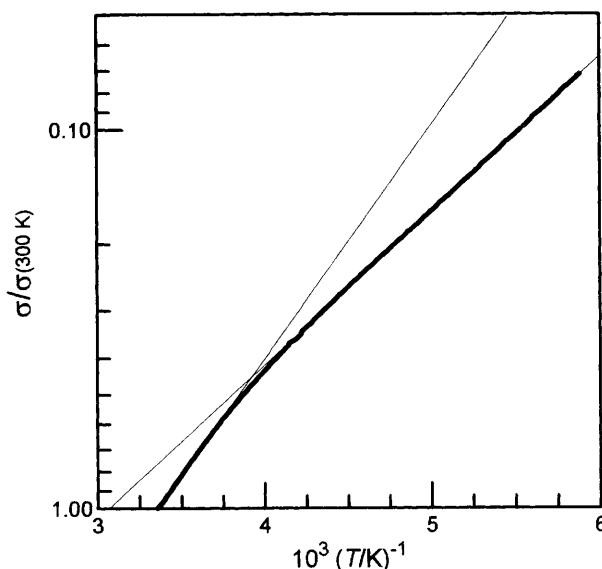


Fig. 5 Logarithmic plot of the conductivity, σ , along the b axis of $[(\text{C}_{20}\text{H}_{12})_3][\text{FeCl}_4]$ as a function of the reciprocal temperature. The thin lines are the linear fits for data above 270 K and below 240 K, respectively

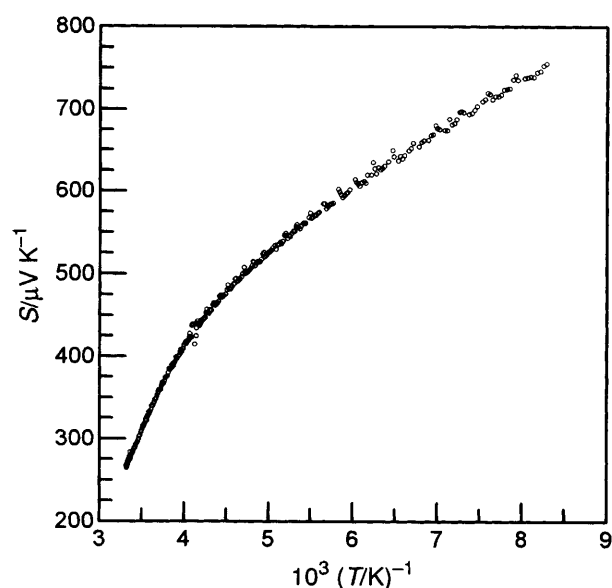


Fig. 6 Absolute thermopower along the *b* axis of $[(C_{20}H_{12})_3][FeCl_4]$ as a function of the reciprocal temperature

Although the analysis of the next-neighbour distances between iron atoms in **1** indicates a closest separation of 7.89 Å, closely followed by separations at 8.33, 9.64 and 10.04 Å, an attempt to fit the susceptibility data by a high-temperature series expansion for a three-dimensional Heisenberg simple cubic $S = \frac{5}{2}$ lattice gave a poorer fit than that obtained by the simple model of interacting pairs of $S = \frac{5}{2}$ spins,²³ with a temperature independent term $N\alpha$ [equation (2)] where J is the exchange constant, N_0 the Avogadro's number and k the Boltzmann constant. A good fit of the data to this function was obtained with values of $J/k = -1.26(1)$ K, $g = 2.022(4)$ and $N\alpha = 0.0011(1)$ emu mol⁻¹ for **1** and $J/k = -3.72(4)$ K, $g = 2.03(2)$ and $N\alpha = 0.0015(5)$ emu mol⁻¹ for **2** as shown in Fig. 7. The agreement with equation (2) is an indication that, although with small J , the exchange pathway between $Fe \cdots Fe^{III}$ via short $Cl(4) \cdots Cl(4^{III})$, contacts is dominant over the remaining ones. A similar situation should occur also in compound **2**.

The g values derived by these fittings are in good agreement with those given by EPR measurements for single crystals. At room temperature the EPR spectra presents almost isotropic lines with g values in the ranges 2.016–2.018 and 2.040–2.045, and widths in the ranges 300–325 and 70–90 G for **1** and **2** respectively. These values are certainly due only to the tetrahalogenoferrate(III) ion, since any contribution due to the perylene cation to susceptibility is expected to be at least three orders of magnitude smaller.

The perylene interplanar distance in **1** (average 3.38 Å) is only slightly larger than that observed in other perylene chain compounds, namely in $[(C_{20}H_{12})_2][M(mnt)_2]$ where distances in the range 3.32–3.36 Å, depending on metal *M*, have been observed.^{3,4,7}

These compounds have regular stacks of perylene molecules with a partial oxidation corresponding to $(C_{20}H_{12})_2^+$ and therefore present metallic properties at high temperatures as expected for a $\frac{3}{4}$ -filled one-dimensional band. Assuming that for compounds **1** and **2** the positive charge lies in the stacked perylene molecules and the flanking ones are neutral, the stoichiometry imposes the same average partial oxidation as in

$\chi_p =$

$$(N_0 g^2 \mu_B^2 / kT) \frac{[55 + 30 \exp(-10J/kT) + 14 \exp(-18J/kT) + 5 \exp(-24J/kT) + \exp(-28J/kT)]}{[11 + 9 \exp(-10J/kT) + 7 \exp(-18J/kT) + 5 \exp(-24J/kT) + 3 \exp(-28J/kT) + \exp(-30J/kT)]} + N\alpha \quad (2)$$

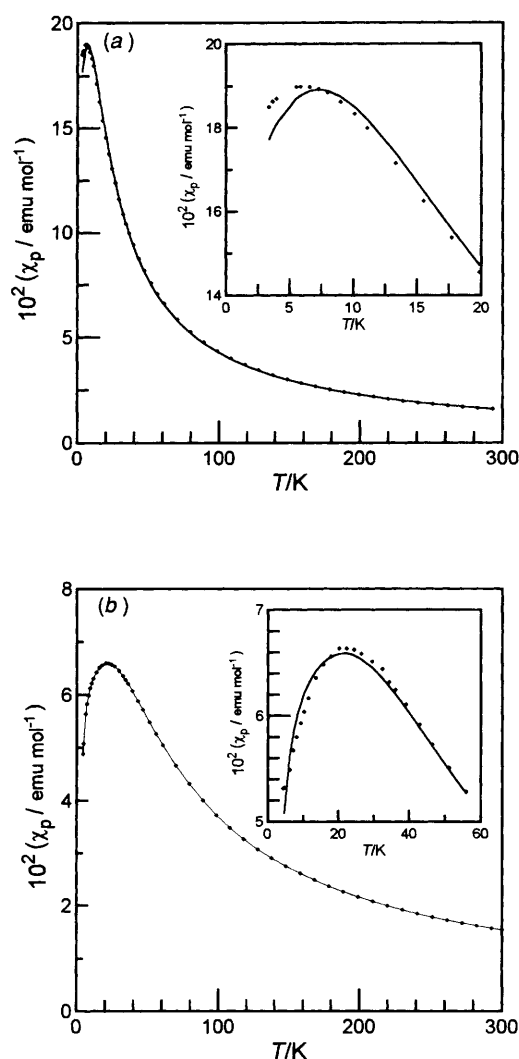


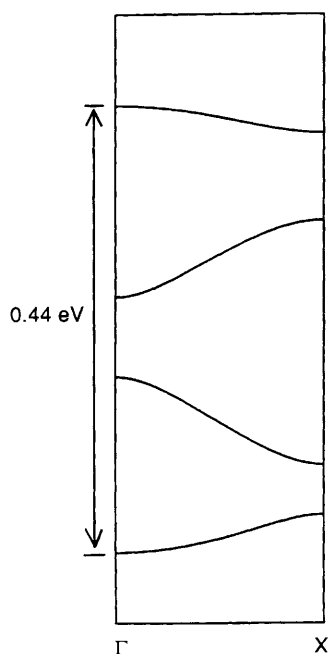
Fig. 7 Paramagnetic susceptibility, χ_p , of (a) $[(C_{20}H_{12})_3][FeCl_4]$ and (b) $[(C_{20}H_{12})_3][FeBr_4]$ as a function of temperature T . The solid lines represent the best fits of equation (2). The insets show in detail the low-temperature region

the $[(C_{20}H_{12})_2][M(mnt)_2]$ compounds. Therefore the semi-conducting properties of **1** are clearly a consequence of the previously described tetramerisation of the perylene stacks due to a transversal displacement of the molecule. The effect of the variation of the overlapping pattern between perylene molecules on the electronic properties has been investigated by extended-Hückel calculations²⁴ with modified H_{ij} values²⁵ and also by the tight-binding approach of the same method.²⁶ The evaluation of the intrastack interactions, and possible interactions between stacked molecules and side perylene molecules were accomplished through the calculations of the interaction energies, $\beta_{ij} = \langle \phi_i | H_{eff} | \phi_j \rangle$,²⁷ between the highest occupied molecular orbitals (HOMOs), ϕ_i , ϕ_j , of each pair of neighbour perylene molecules. Although several side contacts between stacked and side perylene molecules in the range 3.6–3.7 Å exist, due to their almost orthogonal relationship, the corresponding interactions (see Table 5) are very small, between five and twenty meV. These are negligible when compared with

Table 5 Short C...C intermolecular contacts ($d_{CC} < 3.5 \text{ \AA}$) and interaction energies, β , between nearest-neighbour perylene pairs

| Interaction ^a | $d_{CC}/\text{\AA}$ | β_{ij}/meV |
|-----------------------------------|--|-------------------------|
| Contacts along the stacks | | |
| A-B | 3.48, 3.44, 3.47, 3.41, 3.43, 3.38, 3.47, 3.41, 3.49, 3.41, 3.42, 3.44 | 296.3 |
| A-A ^I | 3.42, ^b 3.37, ^b 3.49, ^b 3.48, ^b 3.41, ^b 3.45 ^b | 293.6 |
| B-B ^{II} | 3.39, ^b 3.36, ^b 3.35, ^b 3.39 ^b | 135.4 |
| Side contacts | | |
| B-C ^{VII} | 3.60 ^c | 19.5 |
| A ^I -C ^{VIII} | 3.65 ^c | 13.1 |
| C-D | 3.74 ^c | 4.1 |
| A-D ^{IX} | 3.71 ^c | 9.3 |
| B-D ^{IX} | 3.69 ^c | 4.5 |

^a Symmetry operations: I - $x, 1 - y, 1 - z$; II - $x, 2 - y, 1 - z$; VII $x, 1 + y, z$; VIII $x - 1, y, z$; IX $x, 1 + y, 1 + z$. ^b $2 \times$. ^c Shortest intermolecular C...C distance.

**Fig. 8** Band structure calculated for a perylene stack in the solid $[(C_{20}H_{12})_3][FeCl_4]$; Γ and X are reciprocal space unit-cell coordinates

those between stacked molecules, which range from 135 to 300 meV. These results clearly show that, as expected from the crystal structure, the electronic structure of this solid is one-dimensional. Therefore the band structure corresponding to the stacked molecules was calculated by the tight binding approach. Four bands shown in Fig. 8 were obtained from the HOMO of the four (tetramerised) perylene molecules in the unit cell. Assuming an average oxidation degree corresponding to $(C_{20}H_{12})_2^+$, the Fermi level lies in the middle of the upper gap and therefore semiconducting properties, as experimentally observed, are expected. The calculated gap in this approach is significantly smaller than the experimental gap, a fact that should be indicative of correlation effects not taken into account by the extended-Hückel approach. This four band splitting obtained for this compound contrasts with the simple sinusoidal band with total width of 0.6 eV obtained in the $[(C_{20}H_{12})_2][M(mnt)_2]$ compounds with regular stacks.²⁸ In these compounds the intrastack pair interaction is larger, $> 0.3 \text{ eV}$, and the regular nature of the stack provides a wider band with no gap at the Fermi level.

Acknowledgements

This work was partially supported by the Human Capital and Mobility program of European Communities under contract number CHRX-CT93-0148.

References

- 1 Yu. V. Sushko, T. Ishiguro, S. Horiuchi and G. Saito, *Solid State Commun.*, 1993, **87**, 997; Yu. V. Sushko, I. Hiroshi, T. Ishiguro, S. Horiuchi and G. Saito, *J. Phys. Soc. Jpn.*, 1993, **62**, 3372.
- 2 H. Akamatu, H. Inokuchi and Y. Matsugana, *Nature*, 1954, **173**, 168.
- 3 V. Gama, M. Almeida, R. T. Henriques, I. C. Santos, A. Domingos, S. Ravy and J. P. Pouget, *J. Phys. Chem.*, 1991, **95**, 4263.
- 4 V. Gama, R. T. Henriques, G. Bonfait, L. C. Pereira, J. C. Waerenborgh, I. C. Santos, M. T. Duarte, J. M. P. Cabral and M. Almeida, *Inorg. Chem.*, 1992, **31**, 2598.
- 5 V. Gama, R. T. Henriques, G. Bonfait, M. Almeida, A. Meetsma, S. van Smaalen and J. L. de Boer, *J. Am. Chem. Soc.*, 1992, **114**, 1986.
- 6 V. Gama, R. T. Henriques, G. Bonfait, M. Almeida, S. Ravy, J. P. Pouget and L. Alcácer, *Mol. Cryst. Liq. Cryst.*, 1993, **234**, 171.
- 7 V. Gama, R. T. Henriques, M. Almeida and L. Alcácer, *J. Phys. Chem.*, 1994, **98**, 997.
- 8 L. Alcácer and A. H. Maki, *J. Phys. Chem.*, 1974, **78**, 215; 1976, **80**, 1912.
- 9 M. Y. Ogawa, J. Martisen, S. M. Palmer, J. L. Stanton, J. Tanaka, R. L. Greene, B. M. Hoffman and J. A. Ibers, *J. Am. Chem. Soc.*, 1987, **109**, 1115; M. Y. Ogawa, B. M. Hoffman, S. Lee, M. Yudkowsky and W. P. Halperin, *Phys. Rev. Lett.*, 1986, **57**, 1177.
- 10 M. Y. Ogawa, S. M. Palmer, K. Liou, G. Quirion, J. A. Thompson, M. Poirier and B. M. Hoffman, *Phys. Rev. B*, 1989, **39**, 10682.
- 11 T. Mallah, C. Hollis, S. Bott, M. Kurmoo, P. Day, M. Allan and R. H. Friend, *J. Chem. Soc., Dalton Trans.*, 1990, 859; P. Day, M. Kurmoo, T. Mallah, I. R. Marsden, R. H. Friend, F. L. Pratt, W. Hayes, D. Chasseau, J. Gaultier, G. Bravic and L. Ducasse, *J. Am. Chem. Soc.*, 1992, **114**, 10722.
- 12 J. Raymond, C. Sangster and J. W. Irvine, jun., *J. Chem. Phys.*, 1956, **24**, 670.
- 13 E. M. Engler, R. Greene, P. Haen, Y. Tomkiewicz, K. Mortensen and J. Berendzen, *Mol. Cryst. Liq. Cryst.*, 1982, **79**, 15.
- 14 (a) G. M. Sheldrick, SHELX 86, Program for Crystal Structure Determination, University of Göttingen, 1986; (b) G. M. Sheldrick, SHELX 93, Program for Crystal Structure Determination, University of Göttingen, 1993.
- 15 M. Nardelli, *Comput. Chem.*, 1983, **7**, 95.
- 16 C. K. Johnson, ORTEP II, Report ORNL-3138, Oak Ridge National Laboratory, Oak Ridge, TN, 1976.
- 17 P. E. Schaffer, F. Wudl, G. A. Thomas, J. P. Ferraris and D. O. Cowan, *Solid State Commun.*, 1974, **14**, 347.
- 18 P. M. Chaikin and J. F. Kwak, *Rev. Sci. Instrum.*, 1975, **46**, 218.
- 19 R. P. Huebner, *Phys. Rev.*, 1964, **135**, A1281.
- 20 H. Endres, H. J. Keller, B. Müller and D. Schweitzer, *Acta Crystallogr., Sect. C*, 1985, **41**, 607.

- 21 G. A. Bottomley, A. M. Carter, L. M. Englehardt, F. G. Lincoln, J. M. Patrick and A. H. White, *Aust. J. Chem.*, 1984, **37**, 871; F. A. Cotton and C. A. Murillo, *Inorg. Chem.*, 1975, **14**, 2467; J. A. Zora, K. R. Seddon, P. B. Hitchcock, C. B. Lowe, D. P. Shum and R. L. Carlin, *Inorg. Chem.*, 1990, **29**, 3302.
- 22 H. Fritzsche, *Solid State Commun.*, 1971, **9**, 1813.
- 23 A. P. Ginsberg and M. B. Robin, *Inorg. Chem.*, 1963, **2**, 817.
- 24 R. Hoffmann and W. N. Lipscomb, *J. Chem. Phys.*, 1962, **36**, 2179; 1962, **37**, 2872; R. Hoffmann, *J. Chem. Phys.*, 1963, **39**, 1397.
- 25 J. H. Ammeter, H. B. Bürgi, J. C. Thibeault and R. Hoffmann, *J. Am. Chem. Soc.*, 1978, **100**, 3686.
- 26 M. H. Whangbo and R. Hoffmann, *J. Am. Chem. Soc.*, 1978, **100**, 6093; M. H. Whangbo, W. M. Walsh, jun., R. C. Haddon and E. Wudl, *Solid State Commun.*, 1982, **43**, 637; M. H. Wangbo, J. M. Williams, M. A. Beno and J. R. Dorfman, *J. Am. Chem. Soc.*, 1983, **105**, 645.
- 27 M. H. Wangbo, J. M. Williams, P. C. W. Leung, M. A. Beno, T. J. Emge and H. H. Wang, *Inorg. Chem.*, 1985, **24**, 3500; M. H. Wangbo, J. M. Williams, P. C. W. Leung, M. A. Beno, T. J. Emge, H. H. Wang, K. D. Carlson and G. W. Crabtree, *J. Am. Chem. Soc.*, 1985, **107**, 5815.
- 28 L. F. Veiros, M. J. Calhorda and E. Canadell, *Inorg. Chem.*, 1994, **33**, 4290.

Received 11th May 1995; Paper 5/03013E